Enhanced Fluctuations of the Tunneling Density of States near the Bottom of a Landau Band Measured by a Local Spectrometer

J. P. Holder,[1] A. K. Savchenko,[1] Vladimir I. Fal'ko,[2] B. Jouault,[3] G. Faini,[3] F. Laruelle,[3] and E. Bedel[4]
[1]*Department of Physics, University of Exeter, Stocker Road, Exeter, EX4 4QL, United Kingdom*
[2]*Department of Physics, Lancaster University, Lancaster, LA1 4YB, United Kingdom*
[3]*L2M-CNRS, 196 Avenue H.Ravera, B.P. 107, F-92225 Bagneux, Cedex, France*
[4]*LAAS-CNRS, Toulouse, Cedex, 31077, France*
(Received 29 June 1999)

We have found that the local density of state fluctuations (LDOSF) in a disordered metal, detected using an impurity in the barrier as a spectrometer, undergo enhanced (with respect to Shubnikov–de Haas and de Haas–van Alphen effects) oscillations in strong magnetic fields, $\omega_c\tau \geq 1$. We attribute this to the dominant role of the states near the bottom of Landau bands which give the major contribution to the LDOSF and are most strongly affected by disorder. We also demonstrate that in intermediate fields the LDOSF increase with field B in accordance with the results obtained in the diffusion approximation.

PACS numbers: 73.23.Hk, 72.15.Gd, 73.20.Fz, 73.40.Ty

Resonant tunneling through individual impurities has been identified and studied in vertical [1–4] and lateral [5–7] mesoscopic structures. When an impurity level in a potential barrier passes through the Fermi level in the emitter, it manifests itself as a step in the current-voltage (IV) characteristic, with the magnitude determined by the impurity coupling to the reservoirs and the onset smeared due to the coupling or the thermal distribution of carriers in the contact. With increasing bias, the current onset is followed by a plateau where temperature-independent and magnetic-field-sensitive reproducible features have been observed in several experiments on small-area vertical structures [1,3] which were attributed in [8,9] to the fluctuations in the local density of single-particle states in a disordered emitter [10]. It was suggested [4,8,11] that the impurity carrying the current (spectrometer) can act as a probe of the local density of state fluctuations (LDOSF) in the bulk of metallic contacts. When shifted with a bias, the spectrometer detects a "fingerprint" of the LDOSF as a function of energy.

In this paper, we study the evolution with magnetic field of the LDOSF in a 3D disordered metal, a heavily doped semiconductor, and discuss the results from the point of view of the fluctuation and correlation properties of single-particle wave functions in disordered media. We have measured the fingerprint of the LDOSF, $\delta\nu(\varepsilon)$, in the differential conductance $G(V) = \frac{dI}{dV}(V)$ in a broad range of magnetic fields, B, and analyzed its variance, $\langle\delta G^2\rangle$, and correlation parameters. In intermediate fields, $\omega_c\tau \sim 1$, we have detected an increase of the fluctuation magnitude, in agreement with the theoretically predicted behavior [11]: $\langle(\delta G)^2\rangle_B/\langle(\delta G)^2\rangle_{B=0} \approx 1 + (\omega_c\tau)^2$. At higher fields, $\omega_c\tau \geq 1$, we have observed large $1/B$ periodic oscillations in $\langle\delta G^2\rangle$. We conclude that LDOSF in strong fields are dominated by the states near the minimum of the Landau bands which play a distinguished role relative to the rest of the spectrum. Notably, the observed oscillations are significantly stronger than those in other oscillatory effects in metals, such as de Haas–van Alphen effect.

The investigated structure consists of a 50 Å GaAs well imbedded between two 81 Å $Al_{0.33}Ga_{0.67}As$ barriers. Each Si-doped GaAs contact consists of three layers: 4800 Å with nominal doping 10^{18} cm^{-3} is followed by 4800 Å with 2×10^{17} cm^{-3}, and the latter is separated from the barrier by an undoped spacer of 300 Å and 200 Å, for top and bottom contact, respectively. The lateral area of the nominally undoped quantum well is reduced to a 700 Å diameter disk using the ion bombardment technique [12]. This decreases the number of active impurities in the barrier, thus avoiding overlapping spectra of the LDOSF produced by individual spectrometers. A schematic band diagram of the resonant tunneling device with an impurity level S in the quantum well is shown in the inset of Fig. 1. By testing several samples, we have selected one with a distinct impurity level, which is also well separated from the states of the quantum well which lie about 10 meV above. This energy range determines the interval where the LDOS in the contact can be studied.

At zero bias, the spectrometer level S is above the Fermi level μ of the emitter with 3D metallic conduction. The alignment of S and μ with increasing bias is registered as a step in IV. In the differential conductance $G(V)$ shown in Fig. 1, this current threshold corresponds to a peak at 0.05 V. At low temperatures, its height is $G_\Gamma \simeq \frac{4e^2}{h}\frac{\Gamma_{\max}\Gamma_{\min}}{\Gamma_{\max}^2+\Gamma_{\min}^2} \simeq \frac{4e^2}{h}\frac{\Gamma_{\min}}{\Gamma_{\max}}$ and its width is related to the energetic width of the spectrometer $\Gamma \simeq \Gamma_{\max} \simeq 120$ μeV determined by the tunneling coupling between the impurity and the contacts. The values of $\Gamma_{\min,\max}$ depend on the transparencies of the two barriers, so that $\Gamma_{\max}$ corresponds to the lower (collector) barrier and $\Gamma_{\min}$ corresponds to the higher (emitter) barrier, $\Gamma_{\min} \sim 5 \times 10^{-3}\Gamma_{\max}$, as estimated from the value of G_Γ. The relation between bias V and the energy scale of the spectrometer is established by the coefficientf $\beta = \frac{dE}{d(eV)} = 0.24$, found for the selected

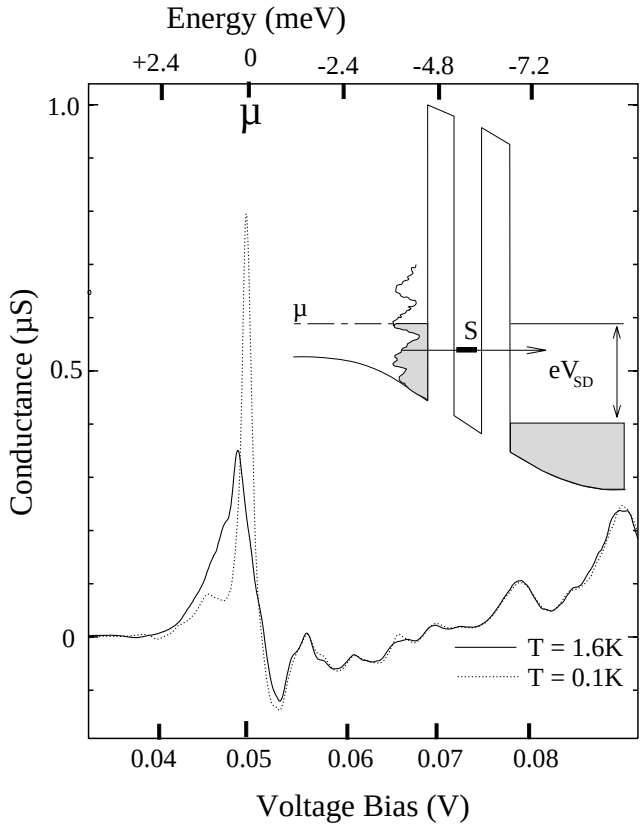

FIG. 1. Differential conductance as a function of bias with the threshold peak and the fingerprint of the LDOS below the Fermi level in the emitter. Inset: band diagram of the resonant tunneling structure with a spectrometer.

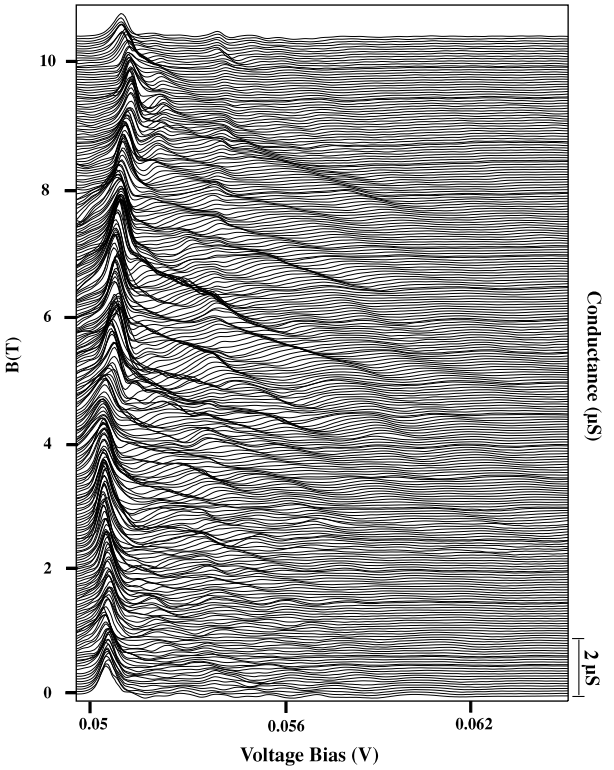

FIG. 2. Conductance fluctuations $G(V, B)$ normalized to the threshold peak. Curves for different B are offset upwards and multiplied by an increasing factor to compensate for the decrease of the threshold peak with field.

structure from the analysis of the temperature smearing of the threshold peak.

Above the threshold, the current is determined by the emitter barrier transparency $\Gamma_{\min}$ and the emitter density of states ν at the energy E_S below the Fermi level. As the barrier height does not change significantly over a small V range, the current becomes a measure of the LDOS in the emitter: $I(V) \propto \nu(E_S)$. Fluctuations with energy of the LDOS give rise to the reproducible, temperature-independent fine-structure in IV. This is seen on top of a smooth decrease in the current reflecting the averaged 3D density of states.

Figure 2 shows the dependence $G(V)$ measured in magnetic fields $0 < B < 10.5$ T applied parallel to the current and changed with a step of 20 mT. Fluctuations $\delta G(V)$ have a correlation voltage of $\Delta V_c \approx 0.5$ mV, which is comparable to the width $\Gamma/e\beta$ of the threshold conductance peak. With increasing magnetic field up to $B \sim 4$ T the fingerprint in $G(V, B)$ changes randomly, with a correlation field $\Delta B_c \sim 0.05$ T. At high fields, the fluctuations transform into a more regular pattern, where individual features, assigned to Landau bands, tend to move with increasing field towards the threshold peak, similar to the observation by Schmidt *et al.* [9].

To interpret fluctuations in $G(V)$ as an image of LDOSF, we employ a picture based on the properties of single-electron wave functions $\psi_i(\mathbf{r})$ in a disordered metal [13–15]. In a phase-coherent 3D metal, the local density of states at a point $\mathbf{r}$ detected by a spectrometer with width Γ can be considered as a sum of local densities, $|\psi_i(\mathbf{r})|^2$, of all eigenstates within energy interval Γ:

$$I(V) \propto \nu(E) \sim \Gamma^{-1} \sum_{|E_S - E_i| < \Gamma} |\psi_i(\mathbf{r})|^2. \qquad (1)$$

The sum in Eq. (1) includes a large number of eigenstates, $N(\Gamma, L) \sim \nu_0 \Gamma L^d$, each of which typically contributing as little as $|\psi(\mathbf{r})|^2 \sim L^{-d}$, with the mean value of the LDOS, ν_0, independent of the sample size L. As far as fluctuations $\delta\nu$ are concerned, one might expect that these fluctuations should vanish upon enlarging the sample, since, for the sum of $N(\Gamma, L)$ independently fluctuating values $\delta|\psi(\mathbf{r})|^2 \sim L^{-d}$, the variance $\langle \delta\nu^2 \rangle$ can be estimated as $N(\Gamma, L)\langle(\delta_L|\psi(\mathbf{r})|^2)^2\rangle$, which is equivalent to $\Gamma^{-2}\nu_0\Gamma L^d L^{-2d} \sim \nu_0 \Gamma^{-1} L^{-d} \to 0$ when $L \to \infty$. However, the correlations between wave functions at close energies make the LDOSF in a large sample finite and independent of its size.

This statement can be explained using Thouless's scaling picture of quantum diffusion [16]. We construct the electron states in a large sample by representing them as linear combinations of wave functions defined in its smaller parts, one of which contains the observation point $\mathbf{r}$, and by gradually combining the smaller parts up to the

actual size L of the sample. For an intermediate length scale ξ of the constituent part, its states are spaced by $\Delta(\xi) \sim (\nu_0 \xi^d)^{-1}$. Diffusive spreading of these states into a larger part, when it is combined with several blocks, leads to their random mixing with the states from the neighboring ξ-size blocks within the Thouless energy $\gamma \sim hD/\xi^2$ [16]; D is the classical diffusion coefficient.

Since at each stage only a finite basis is involved in the construction of the new states, some correlations exist between the new eigenstates, although at small ξ the spread γ is larger than Γ and these correlations are small. However, the Thouless energy γ decreases with increasing ξ, and, for $\xi > L_\Gamma = \sqrt{hD/\Gamma}$, the states will not leave the interval Γ. Thus, L_Γ and $N(\Gamma, L_\Gamma)$ represent the largest length scale and number of states for which correlations between individual eigenfunctions could be neglected and the above estimate of $\langle \delta\nu^2 \rangle$ from independent fluctuators used. Then, for the random difference between two values of ν in the neighboring Γ intervals, one should take $\langle \delta\nu^2 \rangle \sim N(\Gamma, L_\Gamma) \langle (\delta_{L_\Gamma} |\psi(\mathbf{r})|^2)^2 \rangle \sim \nu_0 \Gamma^{-1} L_\Gamma^{-d}$.

The differential conductance is a measure of the derivative, with respect to energy, of the LDOS in Eq. (1), and $\langle \delta G^2 \rangle$ can be taken as $\langle \delta G^2 \rangle \propto \langle \delta\nu^2 \rangle / V_\Gamma^2$. We can normalize the variance $\langle \delta G^2 \rangle$ by the height of the threshold conductance peak determined by the average LDOS and the spectrometer width $V_\Gamma = \Gamma/\beta e$, so that $G_\Gamma \propto N(\Gamma, L_\Gamma) \langle |\psi(\mathbf{r})|^2 \rangle / V_\Gamma$. Then

$$\langle \delta G^2 \rangle / G_\Gamma^2 \approx N(\Gamma, L_\Gamma)^{-1} \approx (\Gamma/hD)^{(d-2)/2} / (\nu hD) \,. \tag{2}$$

We also estimate the correlation voltage of fluctuations as V_Γ and the correlation magnetic field as $\Delta B_c \simeq \Phi_0 / L_\Gamma^2$, where Φ_0 is the flux quantum.

In a 3D system with an anisotropic diffusion tensor (D_x, D_y, D_z), Eq. (2) transforms into $\langle \delta G^2 \rangle / G_\Gamma^2 \propto (D_x D_y D_z)^{-1/2}$. This relation also determines the classical effect on the variance $\langle \delta G^2 \rangle$ of a magnetic field $\mathbf{B} = B\mathbf{l}_z$. Assuming that the cyclotron motion suppresses transverse diffusion as $D_{x,y} = D/[1 + (\omega_c \tau)^2]$ [17–19] gives [11]

$$\langle \delta G^2 \rangle_B / \langle \delta G^2 \rangle_{B=0} \approx 1 + (\omega_c \tau)^2, \qquad \omega_c \tau \lesssim 1 \,. \tag{3}$$

Figure 3 represents the result of our statistical analysis of conductance fluctuations in small magnetic fields. The amplitude of fluctuations is found from an individual $G(V)$ curve at a fixed B in Fig. 2 as $\langle \delta G^2 \rangle = \| [G(B,V) - \|G(B,V)\|]^2 \|$ ($\| \cdots \|$ represents the averaging over range $\Delta V \approx 6$ mV after the threshold peak.) To decrease the scatter, a further averaging over a B range of 0.25 T has been performed. The result is compared to that in Eq. (3). The increase in $\langle \delta G^2 \rangle_B$ agrees with the expected quadratic dependence. From Fig. 3, we find the momentum relaxation time, $\tau \approx 0.9 \times 10^{-13}$ s, and use it to estimate the mobility, $\mu = 0.22$ m^2/V s, in the emitter. The obtained values agree with those expected for the emitter with the same nominal doping [20], and justify our use of the diffusion approximation since $\tau\Gamma/\hbar \sim 10^{-2}$. We also use these values to estimate the zero-field diffusion coefficient, $D \approx 40$ cm^2/V s, and $\Delta B_c \simeq \Gamma/eD \sim 0.03$ T, which is close to the experimental value.

In this experiment we probe the states below the Fermi level, where the concept of quasiparticles may not be applicable, because of the decreased lifetime of the quasiparticle due to electron-electron interactions. However, an estimation of the electron lifetime τ_{ee} [21] shows that the relaxation-induced level broadening, $\hbar/\tau_{ee}$, is much smaller than the energy of the quasiparticles ε, which means that the quasiparticles are well defined. In the energy range where the statistical analysis has been performed, the energy uncertainty is also smaller than Γ. With a further increase of ε (for the range $V \geq 0.058$ in Fig. 2) we have observed an increase of the correlation voltage, which is an indication that the energy spread due to interactions approaches Γ.

Interactions could also induce a singularity in the current near its threshold, as has been observed earlier in experiments with 2D emitters [3]. No sign of the Fermi-edge singularity has been detected in our measurements, which is consistent with the 3D character of the emitter. The 3D nature of the emitter has been directly proved in the experiment with rotating magnetic field, where no significant difference in the fluctuation picture has been detected.

The value of τ confirms that the crossover from weak to strong fields, $\omega_c \tau \sim 1$, takes place at $B \approx 4$ T, where the Landau band (LB) formation is seen in Fig. 2. In the $\omega_c \tau \geq 1$ regime, the field dependence of the variance $\langle \delta G^2 \rangle$ has a strong oscillatory character similar to the de Haas–van Alphen (dHvA) effect, with a sequence of peaks periodic in $1/B$ (Fig. 4a). However, the oscillations in

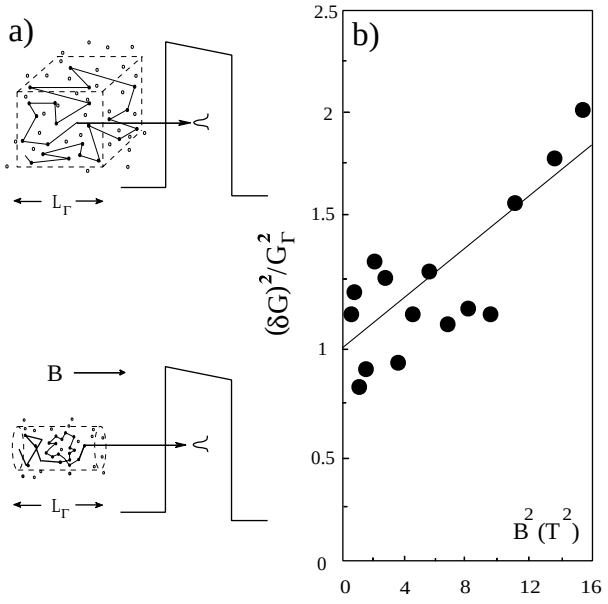

FIG. 3. (a) Diagram of the emitter volume where the tunneling LDOS is formed, at $B = 0$ and $B > 0$. L_Γ is the diffusion length corresponding to electron lifetime h/Γ at the impurity level. (b) Increase of the conductance fluctuations in intermediate fields due to the suppression of transverse diffusion.

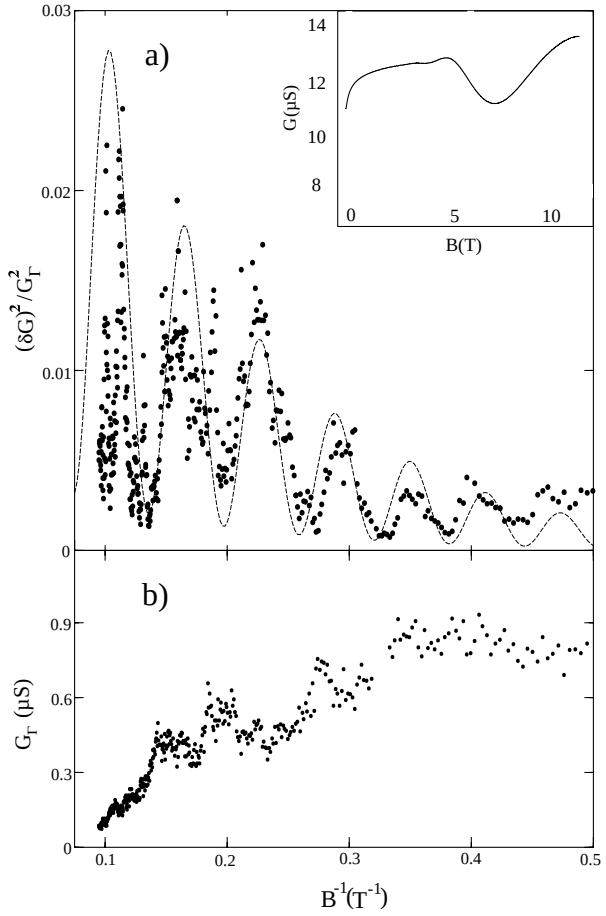

FIG. 4. (a) Oscillations of the conductance variance in strong fields. Inset: SdH oscillations in the bulk conductivity. (b) For comparison, magneto-oscillations of the threshold conductance peak.

$\langle \delta G^2 \rangle$ are much more pronounced than the oscillations in the threshold peak G_Γ, which are due to the modulation of the average density of states at the Fermi level in the emitter caused by depopulation of LB's (Fig. 4b). Also, the observed oscillations look significantly enhanced when compared to the Shubnikov–de Haas (SdH) oscillations of conductance in a lateral GaAs metal semiconductor field effect transistor (MESFET) structure with the same nominal doping as the emitter (Fig. 4a, inset).

These enhanced dHvA-type oscillations in the fluctuation amplitude suggest that the above estimation of $\langle \delta G^2 \rangle$ using statistical properties of typical wave functions should be modified. This can be done by considering a special role of the states with anomalously large fluctuations of a local density, by analogy with [13] where these states were "prelocalized" states. In the case of a smooth random potential with suppressed inter-LB scattering, these anomalous states are the states near the bottoms of LB's. When in strong fields electron motion becomes quasi one dimensional [22], the contribution to the LDOSF from the bottom of the highest filled LB becomes distinguished from typical LDOSF and dominates in the magnitude of the variance $\langle \delta G^2 \rangle$. For energies E_S close to the bottom of the nth LB, $E_n = (n + 1/2)\hbar\omega_c$, not only the transverse but also the longitudinal diffusion coefficient related to the highest LB, $D_z^{(n)} \sim u_z^2 \tau \propto [E_S - E_n]$, are suppressed due to the decrease in the kinetic energy along the magnetic field. When the characteristic length scale $L_\Gamma^z = \sqrt{h D_z^{(n)}/\Gamma}$ becomes smaller than the inter-LB scattering length, the states from the upper LB start providing a contribution $\langle \delta^{(n)} G^2 \rangle$ to the LDOSF that is enhanced compared to the typical variance $\langle \delta^{(\mathrm{typ})} G^2 \rangle$:

$$\langle \delta^{(n)} G^2 \rangle / \langle \delta^{(\mathrm{typ})} G^2 \rangle \approx (\nu^{(n)}/\nu)\,(D_0/D_z^{(n)})^{1/2}. \quad (4)$$

The structure of Eq. (4) explains the enhancement of oscillations in the fluctuation amplitude in Fig. 4 relative to oscillations of $G_\Gamma(B)$ and SdH oscillations. The latter are a measure of the ratio of the LDOS in the highest LB and the total LDOS, i.e., they are represented by the first factor in Eq. (4). The unusual factor $(D_0/D_z^{(n)})^{1/2}$, which is responsible for the enhancement of the oscillations of the fluctuation amplitude, is a specific feature of the LDOSF effect.

We thank I. Lerner, R. J. Haug, T. Schmidt, A. D. Stone, A. Mirlin, and D. G. Polyakov for useful discussions, and EPSRC and NATO for financial support.

[1] B. Su, V. J. Goldman, and J. E. Cunningham, Phys. Rev. B **46**, 7644 (1992).
[2] M. W. Dellow *et al.*, Phys. Rev. Lett. **68**, 1754 (1992).
[3] A. K. Geim *et al.*, Phys. Rev. Lett. **72**, 2061 (1994).
[4] P. J. McDonnell *et al.*, Physica (Amsterdam), **211B**, 433–436 (1995).
[5] A. B. Fowler *et al.*, Phys. Rev. Lett. **57**, 138 (1986).
[6] T. E. Kopley, P. L. McEuen, and R. G. Wheller, Phys. Rev. Lett. **61**, 1654 (1988).
[7] A. K. Savchenko *et al.*, Phys. Rev. B **52**, R17 021 (1995).
[8] T. Schmidt *et al.*, Europhys. Lett. **36**, 61 (1996).
[9] T. Schmidt *et al.*, Phys. Rev. Lett. **78**, 1540 (1997).
[10] I. V. Lerner, Phys. Lett. A **133**, 253 (1988); B. Altshuler, V. Kravtsov, and I. Lerner, *Mesoscopic Phenomena in Solids*, edited by B. L. Altshuler, P. Lee, and R. Webb (North-Holland, Amsterdam, 1991), p. 449.
[11] V. Falko, Phys. Rev. B **56**, 1049 (1997).
[12] G. Faini *et al.*, Surf. Sci. **361/362**, 57 (1996).
[13] V. Falko and K. Efetov, Phys. Rev. B **52**, 17 413 (1995).
[14] A. Mirlin, J. Math. Phys. **38**, 1888 (1997).
[15] Y. Blanter and A. Mirlin, Phys. Rev. B **57**, 4566 (1998).
[16] D. Thouless, Phys. Rev. Lett. **39**, 1167 (1977).
[17] S. Xiong and A. D. Stone, Phys. Rev. Lett. **68**, 3757 (1992).
[18] D. Maslov and D. Loss, Phys. Rev. Lett. **71**, 4222 (1993).
[19] D. Khmelnitskii and M. Yosefin, Surf. Sci. **305**, 507 (1994).
[20] D. A. Poole *et al.*, J. Phys. C **15**, L21 (1982).
[21] B. L. Altshuler, A. G. Aronov, and D. E. Khmelnitskii, J. Phys. C **15**, 7367 (1982).
[22] A. A. Abrikosov and I. A. Ryzkin, Adv. Phys. **27**, 147 (1978); A. A. Abrikosov, J. Low Temp. Phys. **2**, 37 (1970).